TiO2 Microscale Structures

Subjects: Nanoscience & Nanotechnology

Contributor: Vu Khac Hoang Bui , Vinh Van Tran , Ju-Young Moon , Duckshin Park , Young-Chul Lee

TiO_2 microscale structures can be prepared from both TiO_2 precursors and TiO_2 nanoparticles (NPs). TiO_2 microscale structures have many advantages compared to TiO_2 NPs powders, such as tunable structure, higher photocatalytic activity, and ease of recovery. For TiO_2 microscale structures, solid spheres and hollow spheres share some similar synthesis methods. However, microscale TiO_2 microscale structures are not easily mass-produced due to the complexity of the synthesis process.

TiO2 microscale structures solid structures hollow structures photocatalytic

1. TiO_2 Solid Microscale Structures

TiO_2 solid spheres can be synthesized via various methods, such as through addition of surfactants, hydrothermally, spray-drying, freeze-drying, templating, or just by modifying the order of reactant addition.

Different ionic and non-ionic surfactants have been used to synthesize mesoporous materials [1]. Wang et al. (2000) synthesized mesoporous TiO_2 spheres via the slow hydrolysis of titanium alkoxide with neutral surfactant dodecylamine as a template under the condition of environmental humidity. They suggested that the surfactant takes on more important roles in the formation of the mesoporous structure than in the formation of spherical morphologies. In contrast, under low concentrations of titanium tetraisopropoxide $Ti(OPr)_4$, the spherical shapes of TiO_2 are more favorable in the reaction system. The template was removed by diluting 0.3 g of sample in a mixture of ethanol (40 mL) and HCl (1 mL). The presence of an acidified ethanol extraction process is necessary. The obtained TiO_2 mesoporous spheres had a spherical form and smooth surfaces. The sizes of obtained materials ranged from hundreds of nanometers up to several micrometers, with Brunauer–Emmett–Teller (BET) surface areas of 115 m^2/g, specific pore volume of 0.19 cm^3/g, and an average pore diameter of 5.4 nm. They found that static treatment is critical and that the synthesis of TiO_2 materials by stirring or dropping water results in particles lacking specific shape [2].

However, TiO_2 spheres can also be obtained without the use of surfactants or templates. Zhang et al. (2005) prepared both solid TiO_2 spheres (200–300 nm) and hollow TiO_2 spheres (200–500 nm) simply by changing the order of reactant addition. In their preparation of TiO_2 solid spheres, titanium butoxide (TB, 6 mL) was dissolved in absolute ethanol (40 mL). Then, citric acid (0.0015 mol), distilled (DI) water (2 mL), and $NH_3 \bullet H_2O$ (20 mL) were successively added to the above solution. The solution was stirred for several hours and left to stand overnight. Subsequently, the white precipitate was filtered, washed with DI water and ethanol, and dried at 60 °C for 8 h. Lastly, the powder was sintered at 500 °C for 4 h. As for the mesoporous TiO_2 hollow spheres, citric acid (0.0015

mol) was first dissolved in ethanol solution (40 mL) and DI water (2 mL). Afterward, $NH_3 \bullet H_2O$ (10 mL) was added to the mixture solution to form and grow ammonium citrate crystals. Lastly, TB (6 mL) and ammonium (10 mL) were added to the mixture solution at the same time. The dipping rate for ammonia is about two times that of TB. The following steps were the same for both solid and hollow TiO_2 spheres. After the calcination process, the spheres were composed of small particles (7 nm) and formed mesoporous structures (a disordered wormhole framework) that could not be seen before calcination. Zhang et al. (2005) explained that ammonium citrate plays an important role in mesoporous sphere formation, in that mesoporous TiO_2 solid or hollow sphere formation is highly influenced by the extent of TiO_2 condensation that exists at the beginning of ammonium citrate crystal growth. Therefore, they fabricated mesoporous solid spheres simultaneously with the TiO_2 condensation process and the formation of ammonium citrate crystals. In contrast, mesoporous hollow spheres were formed in the presence of ammonium citrate crystal growth and the TiO_2 condensation process, in order (Figure 1). Additionally, both the TiO_2 solid and hollow spheres had a mesoporous structure with average pore sizes of 6.8 and 7.0 nm; and average BET surface areas of 162 and 90 m^2/g, respectively. The bandgap energy values of the TiO_2 solid and hollow spheres were 3.68 and 3.75 eV, respectively [3].

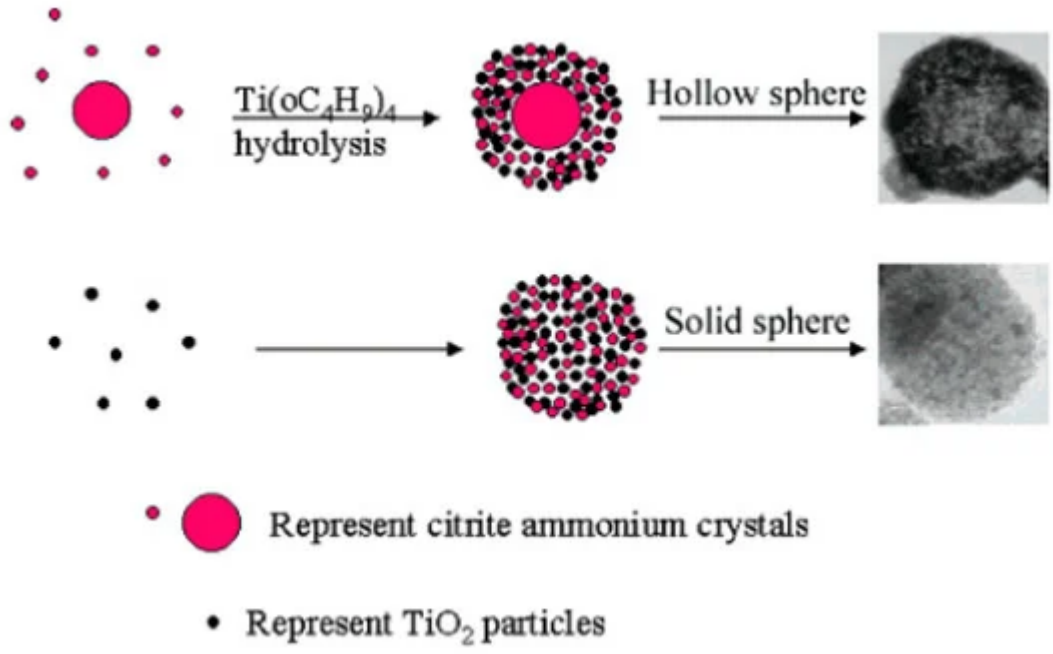

Figure 1. Scheme of mesoporous hollow and solid spheres formation. Reprinted with permission from [3]. Copyright 2005, American Chemistry Society.

The pulsed laser ablation in liquid (PLAL) technique is easy, fast, and eco-friendly. Balati et al. (2019) recently applied the PLAL technique to prepare black titanium dioxide with a TiO_2 rutile microsphere as the core and hydrogenated anatase TiO_2 as the outer layer. The pristine anatase TiO_2 was added into DI water and irradiated with the laser ablation for 5–120 min. The maximum particle size growth was obtained when the sample was irradiated for 120 min. The photocatalytic reaction showed that 99% of methylene blue (MB) was removed after 60 min under visible light irradiation. The enhancement of visible light absorption and the increase of charge carrier

lifetime according to the formation of different types of heterojunctions could be explained by the high photocatalytic performances. In addition, the hydroxyl radical (●OH) was proven to act as the main active species in the photocatalytic reaction [4].

TiO_2 NPs can also be packed into granule form by using the spray-drying method. In spray-drying, a hot gas is used to rapidly dry a NP suspension. Afterward, a spray nozzle is applied to distribute the slurry into a controlled drop-size spray. Vicent et al. (2011) used spray-drying techniques to prepare TiO_2 granules from a P25 nanopowder suspension. The nanosuspension was stabilized by a polyacrylic acid (PAA)-based polyelectrolyte and an ultrasound probe (5 min) was used to increase the solid loading up to 30 vol.%. The obtained granules were spherical and of ~60 µm size and 1335 kg/m^3 density [5]. Faure et al. (2010) used the spray-drying technique to prepare redispersible granules with a size between 20 and 50 µm from TiO_2 NPs. Interestingly, the granules could be converted to TiO_2 NPs with a size distribution similar to TiO_2 powder by ultrasonication [6]. Pal et al. (2014) also used a spray-drying method to prepare TiO_2 microspheres with a diameter of 2 to 10 µm from a hydrothermally cured aqueous suspension of TiO_2 nanoparticles. The obtained TiO_2 microspheres had both anatase and rutile phases. It was shown that the rutile fraction increases with annealing temperature and dominates anatase when the annealing temperature was over 500 °C. Compare with TiO_2 powder, TiO_2 microspheres showed higher photocatalytic activity towards rhodamine B (RhB), MB, and methyl orange (MO). TiO_2 microspheres obtained with an annealing temperature of 400 °C showed the highest degradation efficiency [7].

Vicent et al. (2012) compared TiO_2 granules prepared by freeze-drying and spray-drying. In their study, various parameters such as temperature, pressure, nozzle diameter, and solid loading were evaluated for both methods. They found that only the solids contents of the suspension influenced the morphology and characteristics of dried granules. There were some differences between the TiO_2 granules prepared from freeze-drying and spray-drying. The TiO_2 granules from spray-drying had a monomodal distribution with a higher granule size, while those from freeze-drying were more porous, with a bimodal intragranular distribution. Thus, the TiO_2 granules obtained from spray-drying displayed better flowability (in terms of the Hausner ratio), while those from freeze-drying were softer and of higher porosity [8].

Another popular means of TiO_2 sphere preparation is the hydrothermal or solvothermal method. Du et al. (2011) prepared TiO_2 microspheres using the hydrothermal method under different temperatures (140, 160, 180, and 200 °C) and times (0.5, 2, 24, and 36 h). The temperature condition affected the morphology of the obtained TiO_2 microspheres. At 140 °C, the microspheres were formed with a diameter of about 1–2 µm. When the temperature was increased to 160 °C, the inhomogeneous microspheres were obtained with the largest diameter (~3 µm). At 180 °C, well-defined porous microspheres were obtained and only small ratios of irregular particles could be observed. However, with continued increase of temperature, more irregular particles were seen. The BET surface area of the TiO_2 prepared at 180 °C was five times larger than that of P25 (265.4 m^2/g vs. 50 m^2/g). The optimal reaction time was around 24 h, while the increase of temperature led eventually to the destruction of microsphere structures. The apparent Oswald ripening could be attributed to the formation of the TiO_2 microspheres. In an air purification application, the optimal TiO_2 microspheres (temperature: 180 °C, time: 24 h) could covert 90% of benzene to CO_2 and H_2O after 50 min. In contrast, the removal efficiency for P25 was only 45% under the sample

photocatalytic reaction conditions. In addition, having seen no color change on the surfaces of the TiO_2 microspheres, the authors concluded that the intermediate products had been completely removed from the environment [9].

Mesoporous TiO_2 spheres can be synthesized via hydrothermal methods with sodium salicylate as a template, as was accomplished in a previous study [10]. The as-synthesized TiO_2 was composed of tiny TiO_2 NPs (12–20 nm). With the entrapping of the photosensitizer inside the mesoporous materials, the obtained TiO_2 spheres had photocatalytic activity under the irradiation of visible light. Regarding the formation mechanism of TiO_2 microscale structures via electrostatic interaction, positively charged TiO_2 NPs could react with negative carboxylate groups of sodium salicylate. The presence of the ortho phenolic-OH group in the salicylate molecule formed a supramolecular assembly among the ligated salicylate moieties under mildly acidic synthesis conditions via hydrogen bonding and hydrophobic interactions. This resulted in the formation of the cage-like structure inside the TiO_2 nanocrystals. During the calcination process, the template moieties were removed and mesoporous TiO_2 spheres were formed [10].

Solvothermal synthesis is similar to the hydrothermal methods, but the precursor solution is non-aqueous. Mun et al. (2017) synthesized TiO_2 spheres by solvothermal methods at different temperatures. They observed that the mixed anatase and rutile spheres were collected at 800 °C. At higher temperatures (≥900 °C), the anatase was transferred to the rutile phase. Such spheres have been applied to produce white-light-emitting diodes (WLEDs) with 43.6% higher light extraction efficiency than WLED combinations of commercial YAG:Ce^{3+} and blue LED chips [11].

Recently, Pulido Melian et al. (2019) used the sol–gel method to synthesize TiO_2 microspheres. In their study, TiO_2 microspheres were prepared by hydrolysis and condensation processes from TB precursor and calcinated at 150 °C for 24 h, 400 °C for 1 h, and 630 °C for 1 h. TiO_2 microspheres calcinated at 150 °C had a diameter of 1.25 µm, while both TiO_2 microspheres calcinated at 400 °C and 630 °C had a diameter of 1.75 µm. TiO_2 microspheres were then decorated with Au or Pt particles by photodeposition. They found that TiO_2 microspheres calcinated at 400 °C and modified with Pt (0.27 wt%) showed the highest production rate of hydrogen (2121 µmol/h) [12].

Besides pure TiO_2 solid microscale structures, composite TiO_2 solid microscale structures have been tested. For example, carbon dots (CDs) have been applied to prepare TiO_2 microscale structures due to their good photoelectric properties [13]. Hydroxyl groups and carboxyl groups are formed on the surfaces of CDs that have high water solubility and suitable chemical reactivity [14][15]. By modification of surface groups, the fluorescent properties of such CDs can be controlled [16][17]. In the study by Zhang et al. (2018), CDs were coupled with TiO_2 mesocrystals (CDs/MT), where CDs took the role of both electron collectors and active sites (Figure 2). The 0.75 wt% CDs/MT displayed 5.4 times higher activity than the pure TiO_2 mesocrystals. The loading of CDs did not affect the morphology of the TiO_2 mesocrystals. The CDs/MT of 0.75 wt% retained 60% of its photocatalytic performance after ten cycles, whereas the pure TiO_2 mesocrystals retained only 3% of its photocatalytic performance after five cycles. The 0.75 wt% CDs/MT composite had higher durability and stability due to its positive surface, which is an advantage of the removal of Cr(III) cation through the photocatalytic reaction. The reason for the decrease of

photocatalytic performance after only a few cycles could be explained by the coverage of the active surface sites by photocatalytic reduction products (Cr(III)). Additionally, with the increase of the amount of CDs, the BET, pore volume (V_p), and pore diameter of the TiO_2 microscale structures were slightly reduced. Therefore, the coupling of CDs may cause blockage of pores in TiO_2 mesocrystals. The positive charges on the CD/MT surface play a role in the selective adsorption of Cr(VI) and rapid desorption of Cr(III), thus improving the photocatalytic reduction of Cr(VI) and the retention of photoreduction activity. The pure TiO_2 mesocrystals had a Cr(VI)/Cr(III) adsorption capacity ratio of 7.1, while that for the 0.75 wt% CDs/MT composite was 15. Additionally, the existence of CDs on TiO_2 mesocrystals accelerated the separation of the photogenerated charge. At a pH of 3.0, the 0.75 wt% CDs/MT sample had a zeta-potential of +34.6 mV, higher than the +24.6 mV of the pure TiO_2 mesocrystals. However, the zeta potential was significantly decreased at the pH of 5.0 to ~ + 8.2 mV for the 0.75 wt% CDs/MT sample, and to +20.5 mV for the pure TiO_2 mesocrystals samples. Due to this reduction, the 0.75 wt% CDs/MT sample achieved only 65% photoreduction activity as compared to the pure TiO_2 mesocrystals at the same pH value (5.0) [13].

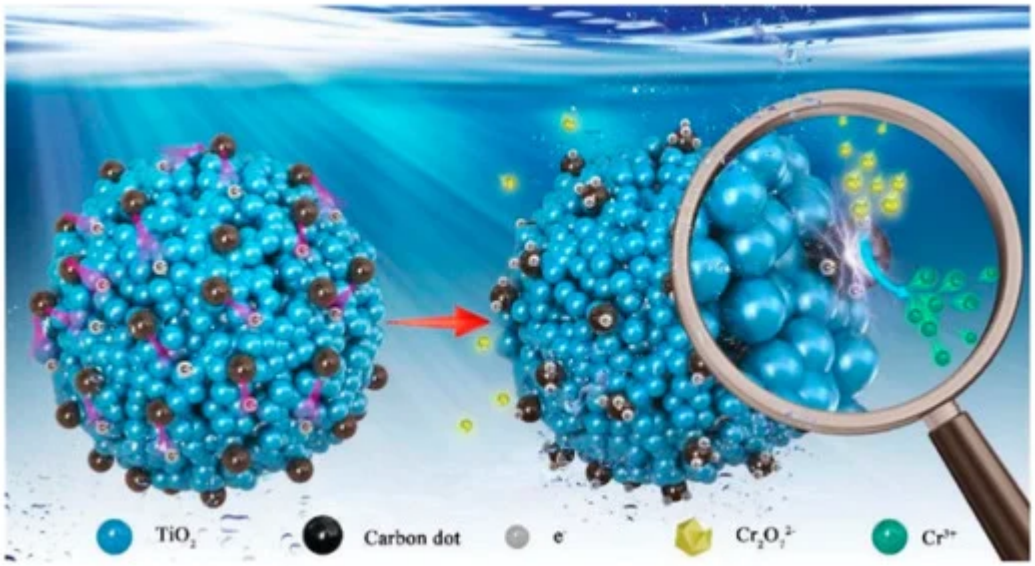

Figure 2. Adsorption–photoreduction–desorption mechanism of Cr(VI) in the presence of the CDs/MT composite. Reprinted with permission from [13]. Copyright 2018, Elsevier.

In addition, TiO_2 NPs have been coated onto different polymers to form TiO_2 microscale structures. According to Singh et al. (2013), the advantages of polymer-support TiO_2 come from the maximal light-utilization efficiency, economic advantages, high degradation efficiency, and easy recovery after photocatalytic reaction [18].

Fabiyi et al. (2000) used a simple thermal treatment method to coat P25 onto expanded polystyrene (PS) for methylene blue (MB) photodegradation. Under thermal treatment (~150 °C), the polystyrene could be expanded 2–4 times larger than its original size, thus lowering its density (from ~0.9 g/cm^3 to ~0.62 g/cm^3). These TiO_2/PS beads could be used to remove MB from an aqueous solution for ten consecutive cycles with a removal efficiency reduced by only about 30%, thus confirming their reuse ability. However, the limitation of this study was the lack of visible light activation of the resulting TiO_2 microscale structures [19].

In the study by Magalhaes et al. (2009), 18 wt% TiO_2 was permanently coated onto expanded polystyrene (EPS). A PS solution (10 wt%) in ethyl acetate (EA) was sprayed onto the EPS particles (1 g, 2–4 mm) and TiO_2 (1 g) was immediately dispersed onto the PS/EA surface. The EA was removed after drying at 80 °C for 1 h and the TiO_2 particles were immobilized on the EPS surface by a rigid PS layer. This floating TiO_2/EPS was used for four consecutive cycles without any significant reduction in dye removal efficiency. Interestingly, the total organic carbon (TOC) removal efficiencies even increased after the first cycle. These authors explained that the enhancement of the TOC removal efficiencies could have come from the “aging” process of the catalysts, whereby in the second cycle the catalyst was wetter and had better interaction with the aqueous surface. The TiO_2 was strongly grafted and could not be removed from the surface of the EPS after 1 h of vigorous stirring in water. However, the surface area of the TiO_2/EPS (4 m^2/g) was lower than the P25 powder (45 m^2/g). Even though TiO_2/EPS had a lower surface area, it was better than the P25 powder in the photocatalytic test. This could be explained by the precipitation of the P25 powder to the bottom of the reactor, which could not be irradiated by ultraviolet (UV) or solar light. Infrared (IR) spectroscopy analysis also confirmed that the EPS surfaces had not been attacked by the generated ROS during photocatalytic degradation [20].

Baek et al. (2013) prepared TiO_2-activated carbon spheres (TiO_2-SAC) by coating of TiO_2 onto strong acid ion exchange resin (Diaon SK1BH) (Figure 3). However, with the high activation temperature (900 °C), the peaks of rutile were shown in a powder X-ray diffraction (XRD) analysis. The anatase crystallite size of the TiO_2-SAC decreased with increasing activation time. Activation time increased the specific surface area and enhanced the porosity. Thus, TiO_2-SAC with activation times of 6 and 9 h (which are mesoporous spheres) showed adsorption towards humic acid and the best photocatalytic performance. The TiO_2-SAC with an activation time of 9 h had the same photocatalytic ability as TiO_2-SAC with an activation time of 6 h, even though it had the highest titanium content (10 wt%) and the largest specific surface area (1427 m^2/g) and total pore volume (1.2 cm^3/g). This phenomenon could be explained by the former’s higher proportions of the rutile phase, as mentioned above. From the inductively coupled plasma optical emission spectroscopy (ICP-OES) analysis, the leaching of titanium into the environment after the photocatalytic reaction was negligible. The TiO_2-SAC spheres exhibited recycling abilities with only a small decrease (~13%) of removal efficiency in the following cycles. By using the exchange method and activation process, TiO_2 can be immobilized onto ion exchange resin without any binder and can maintain a smooth surface (Figure 3) [21].

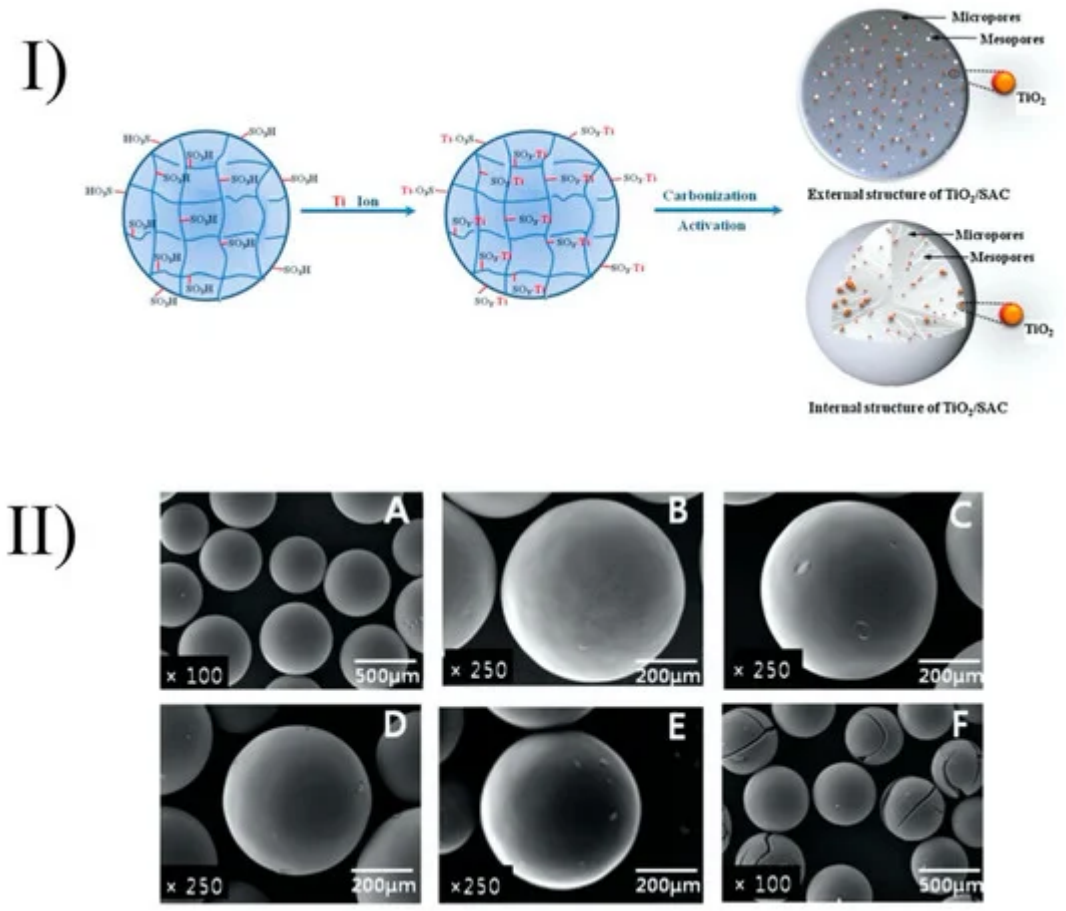

Figure 3. Formation of TiO_2/SAC spheres (**I**) and their surfaces after heat treatment (**II**) at different temperatures: strong acid ion exchange resin (**A**), TiO_2/SAC-700 (**B**), TiO_2/SAC-900–0.5 (**C**), TiO_2/SAC-900-2 (**D**), TiO_2/SAC-900-6 (**E**), and TiO_2/SAC-900-9 (**F**). Reprinted with permission from [21]. Copyright 2013, Elsevier.

Floating structures have some advantages, such as the ability to receive sufficient light energy to produce free radicals [22]. In order to create floating structures, one strategy is the immobilization of TiO_2 NPs onto different substrates, such as hollow glass beads, exfoliated vermiculite, or EPS beads [20][22][23][24]. In addition, floating photocatalytic composite structures can be prepared by injection of lipid (sunflower oil or liquefied cocoa butter) into the TiO_2 suspension to control the size of emulsion via the membrane emulsification process. TiO_2 microscale structures have diameters ranging from 80 to 300 μm. In a previous study, the photocatalytic activity of floating structures was enhanced by the introduction of silver particles. The composite particles based on cocoa butter were shown to be more robust and were not affected by the consequences of the UV photocatalytic reaction. Through the combination of cocoa butter and hexane, the obtained composites floating structures contained 36 mg of TiO_2 per gram of particle. Interestingly, optimal dye decomposition was achieved with a particle surface coverage of between 60 and 80%. Complete surface coverage affected a reduction in photocatalytic activity due to the reflection of UV light [25].

High-speed granulation can be used to convert powder of nanoparticles into micrometer- or millimeter-sized granules. Goedecke et al. (2017) immobilized TiO_2 NPs on the surface of SiO_2 granules using a high shear

granulation process with nanozirconia used as the inorganic binder. TiO_2-coated granules tempered at 300 °C displayed high stability in an aqueous solution up to several hours. The structure with SiO_2 as the core and TiO_2 at the outer layer was confirmed by energy-dispersive X-ray spectroscopy (EDX). From SEM images, the thickness of the TiO_2 layer was around 5–10 µm. Interestingly, the smaller fraction (250–500 µm) with the higher surface area displayed lower photocatalytic activity against MB than the coarse fraction (500–1000 µm). The uneven structure of the TiO_2 layer in the smaller fraction granules explained these results. The photocatalytic of TiO_2-coated granules remained nearly the same after recycling by washing with ultrapure water and drying [26].

Al_2O_3 is a good substrate to coat with TiO_2 to form TiO_2/Al_2O_3 structures [27][28]. For example, Xu et al. (2009) prepared TiO_2/Al_2O_3 microspheres using the sol–spray–calcination method. Briefly, powder TiO_2 NPs (Degussa P25) were mixed with the Al_2O_3 powder in a TiO_2/Al_2O_3 molar ratio of 50:1. Then, a spray layer was used to produce microspheres. The TiO_2/Al_2O_3 microspheres, therefore, were calcined at 500 °C for 3 h. The obtained TiO_2/Al_2O_3 microspheres had a diameter in the range of 20–100 µm with a surface area of 33.86 m^2/g. The TiO_2/Al_2O_3 microspheres showed good photocatalytic activity, whereby 80% of humic acid (HA) was degraded after 140 min. The photocatalytic activity of TiO_2/Al_2O_3 microspheres remained at around 70% after 20 cycles of reuse [28].

TiO_2 could also be coated on the porous activated carbon (AC) to form TiO_2/AC photocatalysts. Arana et al. (2004) coated TiO_2 NPs on the surface of activated carbon (AC) by mixing and stirring with activated carbon (7% *w*/*w*) for 1 h. The obtained TiO_2/AC had a diameter of 6 µm. Compared with bareTiO_2, TiO_2/AC photocatalysts displayed almost no deactivation in any degradation experiments against gas-phase alcohols (methanol, ethanol, 1-propanol, and 1-butanol) [29]. In addition, Ouzzine et al. (2014) used a sol–gel method to coat TiO_2 on the surface of spherical AC. The advantages of spherical activated carbon compared to the powdered and the granular activated carbon come from its smoother surface, better fluidity, and higher mechanical strength. The oxidation treatment at low temperatures is enough to obtain the TiO_2/AC with high photocatalytic activity against propene at low concentration [30].

2. TiO_2 Hollow Microscale Structures

TiO_2 with hollow structures has many advantages, such as improved light scattering and slow photon effects, charge combination suppression, as well as a large number of reactive sites on the surfaces of the shells [31]. A solid structure with an empty side inside a distinct shell can be defined as a “hollow nanostructure”. According to Xiao et al. (2018), hollow-nanostructure TiO_2 has enhanced photocatalytic activities due to the improvement of the harvesting of light energy via light scattering and slow photon effects, the suppression of charge separation by the decrease of charge transfer distance and separation of charge carriers, and the promotion of surface reactions due to a large accessible surface area [31].

There are different ways to synthesize TiO_2 hollow sphere structures: the template-free method, the self-templating method, the soft-templating method, and the hard-templating method (Figure 4) [31]. The details of these synthesis methods, as well as the advantages and disadvantages of TiO_2 hollow nanostructures, can be found in the

outstanding review of Xiao et al. (2018) [31]. In the present review, we introduce only some remarkable examples of the preparation of hollow structures.

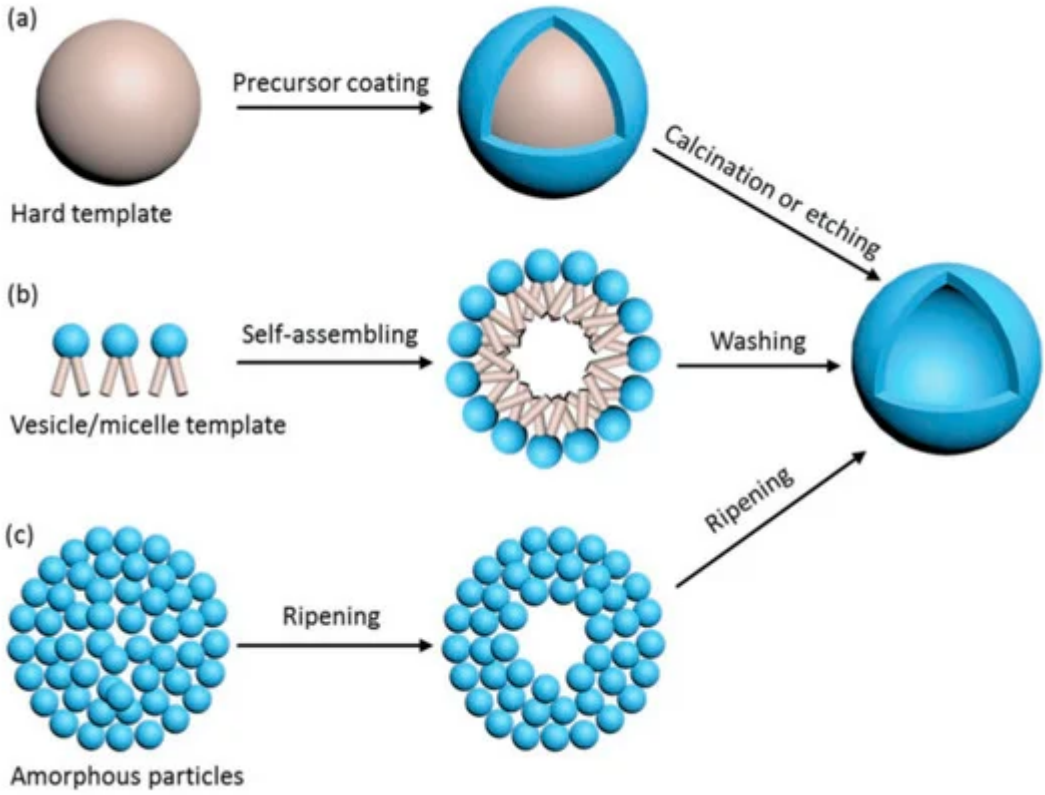

Figure 4. Preparation of TiO_2 hollow spheres via the hard-templating method (**a**), soft-templating method (**b**), and self-templating method (**c**). Reprinted with permission from [31]. Copyright 2018, John Wiley and Sons.

Briefly, in the hard-templating methods, the TiO_2 precursor is coated outside the rigid template and the hollow structure is obtained after the calcination or etching process (Figure 4a). The limitation of these methods is due to the complexity of the template removal process (requiring calcination at high temperature or etching in alkaline and acid solutions) [31]. In soft-templating methods, the formation of hollow nanostructures is achieved via the difference of surface tension at the interfaces, such as water–oil or liquid–gas interfaces (Figure 4b). In most of these cases, removal of the soft template is not required. The limitations of the soft-templating methods derive from the lesser controllability of the shape, the shell thickness, and the size uniformity of the final products [31].

In contrast to the two above-noted synthesis strategies, the self-templating method has attracted interest due to its lower production cost and feasibility for scaling up to the industrial scale. Ostwald ripening is attributed in some papers to the mechanism of the growth of TiO_2 spheres and hollow spheres [32][33]. Ostwald ripening is a thermodynamic process that is tailored by the differences in Gibbs energy (ΔG) between the high G of the precursor and the low G of the resultant hollow nanostructure. A hollow nanostructure can be achieved by the formation of the shell, which is composed of large particles, while the core is left vacant (Figure 4c). Other

remarkable principles entailed in the self-templating of hollow spheres are the Kirkendall effect, galvanic replacement, and surface-protected etching [34][35][36].

Similarly to the case of TiO_2 spheres, the hydrothermal technique can be used to prepare TiO_2 hollow spheres via the self-templating approach. According to Yang et al. (2004), there are two basic types of hollow spheres: type (i) and type (ii) (Figure 5) [32].

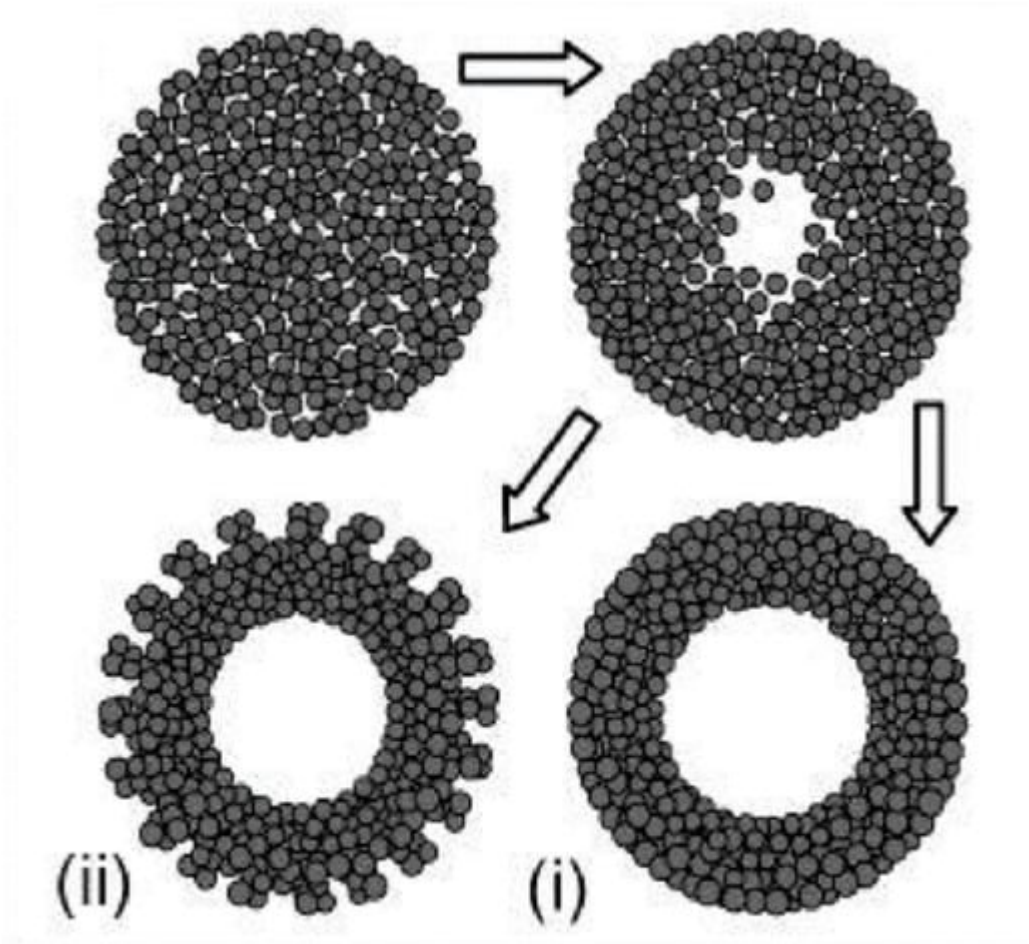

Figure 5. Two types of TiO_2 hollow structures via Oswald ripening by hydrothermal process. Type (**i**) shows a dense and smooth surface, while type (**ii**) displays a less compact surface due to the achieved crystallite extrusion. Reprinted with permission from [32]. Copyright 2004, American Chemical Society.

Yang et al. (2004) prepared hollow anatase TiO_2 spheres via Oswald ripening under hydrothermal conditions. TiO_2 was prepared with titanium tetrafluoride (TiF_4) as a precursor and the hydrothermal process was operated at 140–220 °C for 1.5–100 h. They observed that when the reaction time is short TiO_2 spheres have a solid core, and that hollow spheres are observed when the reaction time is prolonged. The high concentration of TiF_4 imparts a thicker shell due to the higher growth rate. Additionally, different additives have different effects on the growth of a hollow structure. For example, while thiourea can accelerate the hollowing process, the effect of urea is negligible. This can be explained by the difference of chelating abilities between: S = C and :O = C with respect to the titanium

cations, as well as the difference in the chemical natures of their hydrolysis products. The obtained TiO_2 hollow structure has a diameter in the range of 30–50 nm and lengths in the range of 150–250 nm. With 30 mL of TiF_4 at 180 °C for 50 h of reaction time the TiO_2 nanosphere type (i) can be obtained, while the TiO_2 nanosphere type (ii) can be obtained with TiF_4 (30 mL) + thiourea (10 mg) at 180 °C for 10 h. Yang et al. (2004) also concluded that a suitable temperature should be ≥ 160 °C. To obtain hollow TiO_2 spheres, when the temperature reaches 220 °C, the reaction time can be reduced to 5 h [32]. Kang (2012) prepared mesoporous TiO_2 hollow spheres with titanium butoxide (TB) as a precursor via a solvothermal process without the use of any templates or surfactants. The obtained hollow spheres had a specific surface area of 141 m^2/g, a diameter of 700 nm, and a shell thickness of 90 nm. Their photocatalytic degradation of methyl orange (MO) was 98% after 30 min irradiation of UV light (300 W) [37]. Ma et al. (2019) found that TiO_2 hollow spheres can be composed of different nanobuilding blocks by adjusting the starting solution. In detail, the presence of $NH_3 \bullet H_2O$ could lead to TiO_2 hollow microspheres composed of nanoparticles (THPs), the absence of $NH_3 \bullet OH$ could produce TiO_2 hollow microspheres composed of mesoporous nanospheres (THSs), and the hydrothermal treatment in NaOH could result in TiO_2 hollow microspheres composed of nanowires (THWs). The differences in the structure of TiO_2 hollow microspheres could lead to the differences in photocatalytic performances. The THPs showed the lowest photocatalytic activity, while the THSs displayed the highest photocatalytic activity against Rhodamine B (RhB) in the same conditions. The advantages of THPs could be explained by its highest surface areas [38]. Recently, Xie et al. (2019) applied solvothermal to prepare SnO_2/TiO_2 microspheres. The obtained SnO_2/TiO_2 microspheres continued to anneal at 450 °C for 2 h. In the results, microspheres with diameters in the range of 500–1000 nm were assembled with a surface area of 199.3 m^2/g. SnO_2/TiO_2 granules were then utilized as a scattering layer for dye-sensitized solar cells, showing 28.1% improvement of the photovoltaic conversion efficiency when compared with bare nanocrystalline-based cells [39]. The TiO_2 microsphere was also coated with noble metal to improve its photocatalytic performances. Chowhury et al. (2019) decorated gold (Au) nanoparticles on TiO_2 microspheres to degrade phenol under visible light irradiation. They found that the TiO_2 microspheres with 5 wt% Au showed the highest photocatalytic performances, whereby 97% of phenol was removed after irradiation for 1 h by visible light [40].

In comparison with the conventional methods, which localize overheating output from the hot surface of the reaction vessels, possibly leading to product composition changes in cases of heating for elongated periods, the microwave method takes advantage of the potential to produce uniform internal heating by direct coupling of microwave energy with the polar molecules present in the reaction mixture [33]. In order to produce TiO_2 hollow spheres, Alosfur et al. (2018) recently utilized a 100 mL solution of titanium (IV) isopropoxide (TTIP 0.2 M; 95% ethanol) placed in a microwave oven with a reflux device and magnetic stirrers at 550 W for 5 min. Then, the precipitate was centrifuged (4000 rpm for 5 min), dried at 90 °C in air overnight, and calcined at 500 °C for 1 h to obtain anatase TiO_2 hollow spheres. The resultant spheres had sizes in the range of 200 to 500 nm, with pore sizes in the range of 2–50 nm and a surface area of 172.3 m^2/g. The growth mechanism of the TiO_2 hollow spheres was attributed to the Ostwald ripening process during heating. The photocatalytic activity of the TiO_2 hollow spheres for MB was high under both UV and visible light irradiation; this was attributed to the organization of the NPs into a hierarchical structure that can prevent random aggregation [33].

Recently, Balati et al. (2020) used pulsed laser ablation (PLAL) to prepare hydrogenated anatase- and rutile-based inorganic hollow microspheres ($HBTiO_2$/RBIHM). Thus, $HBTiO_2$/RBIHM was decorated with MoS_2 nanosheets ($HBTiO_2$/RBIHM-MoS_2) by microwave irradiation for the visible light arsenic photooxidation. The interconnected layers of MoS_2 resulted in the formation of porous 3D nanostructures in $HBTiO_2$/RBIHM-MoS_2. $HBTiO_2$/RBIHM-MoS_2 could achieve 96.6% arsenite photooxidation efficiency, and 70.3% and 5200 µg/g arsenate adsorption capacity. The synergetic effects from RBIHM-$HBTiO_2$, RBIHM-MoS_2, and $HBTiO_2$/RBIHM heterojunctions explained the performance of $HBTiO_2$/RBIHM-MoS_2 [41].

The soft-templating method is also a popular method used for the preparation of TiO_2 hollow spheres. Similar to TiO_2 solid spheres, different surfactants can be used to synthesize mesoporous TiO_2 spheres with particle sizes ranging from submicrometers to micrometers using dodecyl-amine as a surfactant [42]. In the study by Ren et al. (2003), TiO_2 hollow microspheres were synthesized with poly(ethylene oxide) as a surfactant. The obtained hollow microspheres had a surface area of 0.378 m^2/g, a pore volume of 0.34 cm^3/g, and a pore size of 2.6 nm. The TiO_2 hollow microsphere formation could be explained as follows: the hydrolyzed alkoxides (nanosized Ti-O particles) interacted with amphiphilic surfactant molecules via weak hydrogen bonding, forming mesostructured hybrid inorganic–organic precursory NPs, then gelling to form an -O-Ti-O-Ti- network under autoclaving by polycondensation between NP precursors, finally leading to mesostructured spherical shells. However, the authors stated that the obtained TiO_2 hollow microspheres had an irregular shape due to the lack of complete hydrolysis, and thus could be destroyed in the calcination process. Due to the incomplete condensation, there was a large number of hydroxyl groups on the surfaces of the TiO_2 microspheres. These hydroxyl groups could function as active sites in catalysis or as binding sites for further surface modification [43].

Zhang et al. (2005) used the micelles of salicylic acid (SA) anions and anilinium cations containing TiO_2 for formation of polyaniline (PANI)/TiO_2 microspheres. PANI has been widely applied in the preparation of TiO_2 hollow spheres due to its cheap, simple preparation, uniquely controllable properties via oxidation and protonation states, outstanding environmental stability, and potential application to electronic devices [44]. The molar ratios of aniline (ANI) to SA and ammonium per-sulfate ($(NH_4)_2S_2O_8$), APS) were both 1:1. The PANI-SA microsphere was formed by the hydrogen bond between the -OH group of SA and the amine group of PANI. The PANI/TiO_2 microsphere was believed to have a core–shell structure with TiO_2 as the “core” due to its hydrophobicity and ANI/SA as the “shell” due to the hydrophilicity of the SA dopant (-COOH groups). The polymerization process was expected to occur at the interface of micelle–water due to the hydrophobicity of APS as an oxidant, while the growth of the microspheres was managed by the accretion process [45][46][47][48]. The obtained polyaniline/TiO_2 microspheres (PANI-SA/TiO_2) had an average diameter of around 2.5–3.6 µm, while the thickness of the TiO_2 layer was ~15 nm. The TiO_2 NPs’ position in the composite could be confirmed by water contact angle measurements. TiO_2 NPs are hydrophobic, and so the water contact angle of PANI-SA/TiO_2 was increased to 57.5°, while this number for bare PANI-SA/TiO_2 was 41.2°. However, the water contact angle of PANI-SA/TiO_2 was still lower than that of PANI-β-NSA/TiO_2 nanotubes (β-NSA: β-naphthalenesulfonic acid) prepared by Zhang et al. (2003) in another study. The lower contact angle of PANI-SA/TiO_2 indicated that most of the TiO_2 NPs were filled in the hollow interior of the PANI-SA microspheres [44].

In addition, Zhang and Wan (2003) prepared polyaniline/TiO_2 (PANI-TiO_2) composite nanotubes with diameters in the range of 90–130 nm in the presence of β-naphthalenesulfonic acid (β-NSA). They observed that the morphology of the polyaniline-β-NSA/TiO_2 (PANI-β-NSA/TiO_2) composite was influenced by the TiO_2 concentration. When the TiO_2 concentration was lower than 0.08 M, the PANI-β-NSA/TiO_2 composites formed fibers; but when the concentration was 0.12 M, the morphology of PANI-β-NSA/TiO_2 composites was changed to the granule form. The "core–shell" structure of PANI-β-NSA/TiO_2 was similar to that of PANI-SA/TiO_2 above. However, energy-dispersive X-ray data showed that the TiO_2 NPs were on the walls of the PANI-β-NSA/TiO_2 nanotubes rather than inside of them. This phenomenon was confirmed by the PANI-β-NSA/TiO_2 hydrophobicity (water contact angle: 98.5°) [49].

Gelatin-filled reverse emulsion can also be applied to the preparation of TiO_2 hollow spheres on the nanoscale with water as the polar phase, *n*-dodecane as the non-polar phase, titanium tetrachloride ($TiCl_4$) as a precursor, cetyltrimethylammonium bromide (CTAB) as the surfactant, and 1-hexanol as the co-surfactant. The obtained hollow structures showed an outer diameter of 25–35 nm and a wall thickness of 15–20 nm. Although the TiO_2 hollow spheres were covered by gelatin, their photocatalytic activity was nonetheless similar to that of TiO_2 powder (P25) in their removal of MB (pH = 8) under visible light irradiation [50].

In the hard-templating method, different polymers can be used as the hard template. For example, Wang et al. (2002) prepared hollow shells via the layer-by-layer self-assembly strategy with exfoliated unilamellar titania nanosheets used as inorganic shell building blocks. Spheres of polystyrene (PS) and poly(methyl methacrylate) (PMMA) were used as colloidal templates, and while adjusting the surface charge of these spheres, polyethylenimine was applied. The TiO_2 shell thickness could be adjusted by coating cycles. The polymer core was removed via the calcination process at 500 °C or by UV-irradiation, thereby obtaining titania hollow shells with a smooth surface and small thickness (~5 nm). UV irradiation is a "green" technique by which low temperature is applied to remove the polymer template [51][52]. Interestingly, different treatments, therefore, lead to differences in the optical properties of titania hollow spheres. In another study, the ultraviolet-visible (UV-vis) spectra of calcined hollow spheres were red-shifted compared to UV-irradiated hollow spheres. The transformation of nanosheets with a molecular thickness to the anatase phase could explain the visible differences [53].

Syoufian et al. (2007) applied sulfonated PS latex particles as a hard template in order to prepare submicrometer-sized titania hollow spheres. Titania-PS composites were calcined at 400 °C to remove the template and form TiO_2 hollow spheres. The authors found that the low titanium butoxide (TB) concentration could lead to the formation of hollow spheres with a fragile shell. In contrast, the high TB concentration could result in a relatively smooth and rigid shell. Additionally, when the TB concentrations were 0.15, 0.20, 0.25, and 0.50 M, the shell thicknesses of the titania hollow spheres were 9, 14, 17, and 23 nm, respectively, while their void sizes were 147, 151, 155 and 159 nm, respectively [54]. Hollow spheres synthesized from 0.20 M of TB have the highest anatase phase. In another study, this time on the photodecomposition of MB under the irradiation of a 150 W xenon lamp, the reaction rate was increased two times by the injection of peroxydisulfate as an electron scavenger at an optimal concentration (10 mM). The enhancements of the photocatalytic reaction by electron acceptors can be explained in different ways: (i) the prevention of the recombination of electron–hole pairs by acceptance of the electron from the conduction band, (ii) the increase of the concentration of hydroxyl radical (●OH), and (iii) the generation of other

oxidizing species (e.g., $\bullet SO_4^-$) to promote the intermediate compound oxidation rate [55][56][57]. Further increase of peroxydisulfate leads to saturation of the reaction rate due to excess amounts of SO_4^{2-} species [24].

SiO_2 can also be a candidate for the hard-templating method. One strategy to shift the TiO_2 photocatalytic activity towards the visible region is the combination with narrower bandgap semiconductors, such as cadmium sulfide (CdS) [58][59]. Sue et al. (2014) used the sonochemical method to synthesize a CdS-TiO_2 hollow structure. First, a TiO_2 nanolayer was coated on the surface of SiO_2 via the hydrolysis of TB in DI water under vigorous stirring. Then, CdS was deposited on the SiO_2-TiO_2 core–shell structure via the sonochemical process. SiO_2 was removed via the addition of NaOH, thus forming the CdS-TiO_2 hollow structure. The obtained structures have an average diameter of 300 nm, with the thickness of the TiO_2 shells being about 30 nm, and the diameter of the voids being about 237 nm. Compared with the pure TiO_2 samples, the UV-vis diffuse spectra of the CdS-TiO_2 hollow structure was shifted to the visible light region. With rhodamine B (RhB), >90% of pollutants was removed by the CdS-TiO_2 hollow structure after 120 min under visible light irradiation, more so than other samples, such as P25, CdS, and SiO_2-TiO_2. However, after three cycles of the photocatalytic reaction, the degradation efficiency of the CdS-TiO_2 hollow structure was reduced to ~30%. This reduction was attributed to the photocorrosion of CdS, as well as the mass loss of the catalyst [60].

Besides the above strategies, TiO_2 hollow microspheres can be prepared by spray-drying of an exfoliated titanate sheet suspension without the assistance of any templates. Afterward, the spray-dried gel is calcined at 650 °C/h to destroy the lamellar structure and promote the growth of TiO_2 anatase. The obtained TiO_2 hollow spheres are 10 to 50 μm in size and have a shell thickness of 0.1 μm [61].

There are some differences between TiO_2 dense microscale structures and TiO_2 hollow microscale structures. For the same diameter, titania hollow spheres have a lower density and larger surface area compared with TiO_2 dense spheres [62]. Additionally, compared with TiO_2 dense spheres, the UV absorption spectra of hollow spheres show redshift [63]. This redshift could come from oxygen defects during the formation of TiO_2 particles or by the doping of C or S atoms into TiO_2 particles [63][64][65][66][67].

In both TiO_2 solid and hollow microscale structures, there are still many challenges that remain, notwithstanding their advantages. Firstly, the photocatalytic mechanism of these materials is not fully understood. Secondly, the complexity of synthesis methods also prevents industrial applications of TiO_2 solid and hollow spheres. Besides, the fabrication of these materials with both high crystallinity and large surface areas is still a major challenge. For TiO_2 hollow spheres, the effects of morphological variations of shape, diameter, shell thickness, and numbers of shells should be further investigated [31].

References

1. Meynen, V.; Cool, P.; Vansant, E.F. Verified syntheses of mesoporous materials. Micropor. Mesopor. Mater. 2009, 125, 170–223.

2. Wang, L.; Tomura, S.; Maeda, M.; Ohashi, F.; Inukai, K.; Suzuki, M. Synthesis of mesoporous TiO2 spheres under static condition. Chem. Lett. 2000, 29, 1414–1415.
3. Zhang, Y.; Li, G.; Wu, Y.; Luo, Y.; Zhang, L. The formation of mesoporous TiO2 spheres via a facile chemical process. J. Phys. Chem. B 2005, 109, 5478–5481.
4. Balati, A.; Tek, S.; Nash, K.; Shipley, H. Nanoarchitecture of TiO2 microspheres with expanded lattice interlayers and its heterojunction to the laser modified black TiO2 using pulsed laser ablation in liquid with improved photocatalytic performance under visible light irradiation. J. Colloid Interface Sci. 2019, 541, 234–248.
5. Vicent, M.; Sánchez, E.; Santacruz, I.; Moreno, R. Dispersion of TiO2 nanopowders to obtain homogeneous nanostructured granules by spray-drying. J. Eur. Ceram. Soc. 2011, 31, 1413–1419.
6. Faure, B.; Sæderup Lindeløv, J.; Wahlberg, M.; Adkins, N.; Jackson, P.; Bergström, L. Spray drying of TiO2 nanoparticles into redispersible granules. Powder Technol. 2010, 203, 384–388.
7. Pal, S.; Laera, A.M.; Licciulli, A.; Catalano, M.; Taurino, A. Biphase tio2 microspheres with enhanced photocatalytic activity. Ind. Eng. Chem. Res. 2014, 53, 7931–7938.
8. Vicent, M.; Sánchez, E.; Molina, T.; Nieto, M.I.; Moreno, R. Comparison of freeze drying and spray drying to obtain porous nanostructured granules from nanosized suspensions. J. Eur. Ceram. Soc. 2012, 32, 1019–1028.
9. Du, J.; Chen, W.; Zhang, C.; Liu, Y.; Zhao, C.; Dai, Y. Hydrothermal synthesis of porous TiO2 microspheres and their photocatalytic degradation of gaseous benzene. Chem. Eng. J. 2011, 170, 53–58.
10. Patra, A.K.; Das, S.K.; Bhaumik, A. Self-assembled mesporous TiO2 spherical nanoparticles by a new templating pathways and its enhanced photoconductivity in the presence of an organic dye. J. Mater. Chem. 2011, 21, 3925–3930.
11. Mun, J.Y.; Park, J.Y.; Kwak, M.; Moon, B.K.; Jang, K.; Yang, H.K. Synthesis of TiO2 spheres and their utilization in the enhancement light-extraction efficiency of wleds. Mater. Res. Bull. 2017, 94, 456–462.
12. Pulido Melián, E.; Nereida Suárez, M.; Jardiel, T.; Calatayud, D.G.; del Campo, A.; Doña-Rodríguez, J.M.; Araña, J.; González Díaz, O.M. Highly photoactive TiO2 microspheres for photocatalytic production of hydrogen. Int. J. Hydrog. Energy 2019, 44, 24653–24666.
13. Zhang, Y.; Xu, M.; Li, H.; Ge, H.; Bian, Z. The enhanced photoreduction of Cr(VI) to Cr(III) using carbon dots coupled TiO2 mesocrystals. Appl. Catal. B Environ. 2018, 226, 213–219.
14. Zhang, L.-W.; Fu, H.-B.; Zhu, Y.-F. Efficient TiO2 photocatalysts from surface hybridization of TiO2 particles with graphite-like carbon. Adv. Funct. Mater. 2008, 18, 2180–2189.

15. Li, H.; Kang, Z.; Liu, Y.; Lee, S.-T. Carbon nanodots: Synthesis, properties and applications. J. Mater. Chem. 2012, 22, 24230–24253.
16. Baker, S.N.; Baker, G.A. Luminescent carbon nanodots: Emergent nanolights. Angew. Chem. Int. Edit. 2010, 49, 6726–6744.
17. Zheng, X.T.; Ananthanarayanan, A.; Luo, K.Q.; Chen, P. Glowing graphene quantum dots and carbon dots: Properties, syntheses, and biological applications. Small 2015, 11, 1620–1636.
18. Singh, S.; Mahalingam, H.; Singh, P.K. Polymer-supported titanium dioxide photocatalysts for environmental remediation: A review. Appl. Catal. A Gen. 2013, 462, 178–195.
19. Fabiyi, M.E.; Skelton, R.L. Photocatalytic mineralisation of methylene blue using buoyant TiO2-coated polystyrene beads. J. Photochem. Photobiol. A 2000, 132, 121–128.
20. Magalhães, F.; Lago, R.M. Floating photocatalysts based on TiO2 grafted on expanded polystyrene beads for the solar degradation of dyes. Sol. Energy 2009, 83, 1521–1526.
21. Baek, M.-H.; Jung, W.-C.; Yoon, J.-W.; Hong, J.-S.; Lee, Y.-S.; Suh, J.-K. Preparation, characterization and photocatalytic activity evaluation of micro- and mesoporous TiO2/spherical activated carbon. J. Ind. Eng. Chem. 2013, 19, 469–477.
22. Rosenberg, I.; Brock, J.R.; Heller, A. Collection optics of TiO2 photocatalyst on hollow glass microbeads floating on oil slicks. J. Phys. Chem. A 1992, 96, 3423–3428.
23. Berry, R.J.; Mueller, M.R. Photocatalytic decomposition of crude oil slicks using TiO2 on a floating substrate. Microchem. J. 1994, 50, 28–32.
24. Syoufian, A.; Nakashima, K. Degradation of methylene blue in aqueous dispersion of hollow titania photocatalyst: Optimization of reaction by peroxydisulfate electron scavenger. J. Colloid Interface Sci. 2007, 313, 213–218.
25. Holdich, R.G.; Ipek, I.Y.; Lazrigh, M.; Shama, G. Production and evaluation of floating photocatalytic composite particles formed using pickering emulsions and membrane emulsification. Ind. Eng. Chem. Res. 2012, 51, 12509–12516.
26. Goedecke, C.; Sojref, R.; Nguyen, T.Y.; Piechotta, C. Immobilization of photocatalytically active TiO2 nanopowder by high shear granulation. Powder Technol. 2017, 318, 465–470.
27. Shelimov, B.N.; Tolkachev, N.N.; Tkachenko, O.P.; Baeva, G.N.; Klementiev, K.V.; Stakheev, A.Y.; Kazansky, V.B. Enhancement effect of TiO2 dispersion over alumina on the photocatalytic removal of NOx admixtures from O2-N2 flow. J. Photochem. Photobiol. A 2008, 195, 81–88.
28. Xu, S.; Zhang, X.; Ng, J.; Sun, D.D. Preparation and application of TiO2/Al2O3 microspherical photocatalyst for water treatment. Water Sci. Technol. Water Supply 2009, 9, 39–44.

29. Araña, J.; Doña-Rodríguez, J.M.; Cabo, C.G.I.; González-Díaz, O.; Herrera-Melián, J.A.; Pérez-Peña, J. Ftir study of gas-phase alcohols photocatalytic degradation with TiO2 and AC-TiO2. Appl. Catal. B Environ. 2004, 53, 221–232.
30. Ouzzine, M.; Romero-Anaya, A.J.; Lillo-Ródenas, M.A.; Linares-Solano, A. Spherical activated carbon as an enhanced support for TiO2/AC photocatalysts. Carbon 2014, 67, 104–118.
31. Xiao, M.; Wang, Z.; Lyu, M.; Luo, B.; Wang, S.; Liu, G.; Cheng, H.M.; Wang, L. Hollow nanostructures for photocatalysis: Advantages and challenges. Adv. Mater. 2018, 31, 1801369.
32. Yang, H.G.; Zeng, H.C. Preparation of hollow anatase TiO2 nanospheres via Ostwald ripening. J. Phys. Chem. B 2004, 108, 3492–3495.
33. Alosfur, F.K.M.; Ridha, N.J.; Jumali, M.H.H.; Radiman, S. One-step formation of TiO2 hollow spheres via a facile microwave-assisted process for photocatalytic activity. Nanotechnology 2018, 29, 145707.
34. Skrabalak, S.E.; Au, L.; Li, X.; Xia, Y. Facile synthesis of Ag nanocubes and Au nanocages. Nat. Protoc. 2007, 2, 2182–2190.
35. Zhang, Q.; Zhang, T.; Ge, J.; Yin, Y. Permeable silica shell through surface-protected etching. Nano Lett. 2008, 8, 2867–2871.
36. Cheng, H.; Huang, B.; Liu, Y.; Wang, Z.; Qin, X.; Zhang, X.; Dai, Y. An anion exchange approach to Bi2WO6 hollow microspheres with efficient visible light photocatalytic reduction of CO2 to methanol. Chem. Commun. 2012, 48, 9729–9731.
37. Kang, S.; Yin, D.; Li, X.; Li, L.; Mu, J. One-pot template-free preparation of mesoporous TiO2 hollow spheres and their photocatalytic activity. Mater. Res. Bull. 2012, 47, 3065–3069.
38. Ma, X.; Wang, X.; Yu, C.; Song, Y.; Liang, J.; Min, Q.; Zhang, F. Effects of primary nanobuilding blocks on the photocatalytic performance of TiO2 hierarchical hollow microspheres. J. Alloys Compd. 2019, 773, 352–360.
39. Xie, F.; Wang, J.; Li, Y.; Dou, J.; Wei, M. One-step synthesis of hierarchical SnO2/TiO2 composite hollow microspheres as an efficient scattering layer for dye-sensitized solar cells. Electrochim. Acta 2019, 296, 142–148.
40. Chowdhury, I.H.; Roy, M.; Kundu, S.; Naskar, M.K. TiO2 hollow microspheres impregnated with biogenic gold nanoparticles for the efficient visible light-induced photodegradation of phenol. J. Phys. Chem. Solids 2019, 129, 329–339.
41. Balati, A.; Matta, A.; Nash, K.; Shipley, H.J. Heterojunction of vertically aligned MoS2 layers to hydrogenated black TiO2 and rutile based inorganic hollow microspheres for the highly enhanced visible light arsenic photooxidation. Compos. Part B Eng. 2020, 185, 107785.

42. Wang, Y.; Tang, X.; Yin, L.; Huang, W.; Hacohen, Y.R.; Gedanken, A. Sonochemical synthesis of mesoporous titanium oxide with wormhole-like framework structures. Adv. Mater. 2000, 12, 1183–1186.
43. Ren, T.-Z.; Yuan, Z.-Y.; Su, B.-L. Surfactant-assisted preparation of hollow microspheres of mesoporous TiO2. Chem. Phys. Lett. 2003, 374, 170–175.
44. Zhang, L.; Wan, M.; Wei, Y. Polyaniline/TiO2 microspheres prepared by a template-free method. Synthetic Met. 2005, 151, 1–5.
45. Fuhrhop, J.H.; Helfrich, W. Fluid and solid fibers made of lipid molecular bilayers. Chem. Rev. 1993, 93, 1565–1582.
46. Kim, B.J.; Oh, S.G.; Han, M.G.; Im, S.S. Preparation of polyaniline nanoparticles in micellar solutions as polymerization medium. Langmuir 2000, 16, 5841–5845.
47. Wei, Z.; Zhang, Z.; Wan, M. Formation mechanism of self-assembled polyaniline micro/nanotubes. Langmuir 2002, 18, 917–921.
48. Zhang, Z.; Wei, Z.; Wan, M. Nanostructures of polyaniline doped with inorganic acids. Macromolecules 2002, 35, 5937–5942.
49. Zhang, L.; Wan, M. Polyaniline/TiO2 composite nanotubes. J. Phys. Chem. B 2003, 107, 6748–6753.
50. Zurmühl, C.; Popescu, R.; Gerthsen, D.; Feldmann, C. Microemulsion-based synthesis of nanoscale TiO2 hollow spheres. Solid State Sci. 2011, 13, 1505–1509.
51. Hozumi, A.; Yokogawa, Y.; Kameyama, T.; Hiraku, K.; Sugimura, H.; Takai, O.; Okido, M. Photocalcination of mesoporous silica films using vacuum ultraviolet light. Adv. Mater. 2000, 12, 985–987.
52. Thurn-Albrecht, T.; Schotter, J.; Kastle, G.A.; Emley, N.; Shibauchi, T.; Krusin-Elbaum, L.; Guarini, K.; Black, C.T.; Tuominen, M.T.; Russell, T.P. Ultrahigh-density nanowire arrays grown in self-assembled diblock copolymer templates. Science 2000, 290, 2126–2129.
53. Wang, L.; Sasaki, T.; Ebina, Y.; Kurashima, K.; Watanabe, M. Fabrication of controllable ultrathin hollow shells by layer-by-layer assembly of exfoliated titania nanosheets on polymer templates. Chem. Mater. 2002, 14, 4827–4832.
54. Syoufian, A.; Inoue, Y.; Yada, M.; Nakashima, K. Preparation of submicrometer-sized titania hollow spheres by templating sulfonated polystyrene latex particles. Mater. Lett. 2007, 61, 1572–1575.
55. Wang, Y.; Hong, C.-S. Effect of hydrogen peroxide, periodate and persulfate on photocatalysis of 2-chlorobiphenyl in aqueous TiO2 suspensions. Water Res. 1999, 33, 2031–2036.

56. Irmak, S.; Kusvuran, E.; Erbatur, O. Degradation of 4-chloro-2-methylphenol in aqueous solution by UV irradiation in the presence of titanium dioxide. Appl. Catal. B Environ. 2004, 54, 85–91.
57. Muruganandham, M.; Swaminathan, M. Photocatalytic decolourisation and degradation of reactive orange 4 by TiO2-UV process. Dyes Pig. 2006, 68, 133–142.
58. Liu, Y.; Zhou, L.; Hu, Y.; Guo, C.; Qian, H.; Zhang, F.; Lou, X.W. Magnetic-field induced formation of 1D Fe3O4/C/Cds coaxial nanochains as highly efficient and reusable photocatalysts for water treatment. J. Mater. Chem. 2011, 21, 18359–18364.
59. Meng, H.L.; Cui, C.; Shen, H.L.; Liang, D.Y.; Xue, Y.Z.; Li, P.G.; Tang, W.H. Synthesis and photocatalytic activity of TiO2@Cds and Cds@TiO2 double-shelled hollow spheres. J. Alloys Compd. 2012, 527, 30–35.
60. Xue, C.; Wang, T.; Yang, G.; Yang, B.; Ding, S. A facile strategy for the synthesis of hierarchical TiO2/Cds hollow sphere heterostructures with excellent visible light activity. J. Mater. Chem. A 2014, 2, 7674–7679.
61. Iida, M.; Sasaki, T.; Watanabe, M. Titanium dioxide hollow microspheres with an extremely thin shell. Chem. Mater. 1998, 10, 3780–3782.
62. McDonald, C.J.; Devon, M.J. Hollow latex particles: Synthesis and applications. Adv. Colloid Interface Sci. 2002, 99, 181–213.
63. Ohno, T.; Akiyoshi, M.; Umebayashi, T.; Asai, K.; Mitsui, T.; Matsumura, M. Preparation of S-doped TiO2 photocatalysts and their photocatalytic activities under visible light. Appl. Catal. A Gen. 2004, 265, 115–121.
64. Umebayashi, T.; Yamaki, T.; Itoh, H.; Asai, K. Band gap narrowing of titanium dioxide by sulfur doping. Appl. Phys. Lett. 2002, 81, 454–456.
65. Martyanov, I.N.; Uma, S.; Rodrigues, S.; Klabunde, K.J. Structural defects cause TiO2-based photocatalysts to be active in visible light. Chem. Commun. 2004, 21, 2476–2477.
66. Irie, H.; Washizuka, S.; Hashimoto, K. Hydrophilicity on carbon-doped TiO2 thin films under visible light. Thin Solid Films 2006, 510, 21–25.
67. Syoufian, A.; Satriya, O.H.; Nakashima, K. Photocatalytic activity of titania hollow spheres: Photodecomposition of methylene blue as a target molecule. Catal. Commun. 2007, 8, 755–759.

Retrieved from https://encyclopedia.pub/entry/history/show/7039